Photoluminescence Fatigue and Inhomogeneous Line Broadening in Semi-Insulating Tl_6SeI_4 Single Crystals

S. S. Kostina[1], J. A. Peters[1,2], W. Lin[3], P. Chen[1], Z. Liu[1], P. L. Wang[3], M. G. Kanatzidis[1,3], and B. W. Wessels[1]

[1]*Department of Materials Science and Engineering, Northwestern University, Evanston, IL, USA*

[2]*Department of Chemistry and Physics, Chicago State University, Chicago, IL, USA*

[3]*Department of Chemistry, Northwestern University, Evanston, IL, USA*

Abstract

Photoluminescence (PL) properties of semi-insulating Tl_6SeI_4 have been investigated. A broad emission band centered at 1.63 ± 0.02 eV was observed in all samples. The PL emission band is excitonic in nature and is tentatively attributed to bound exciton emission. PL fatigue (a reduction in PL intensity under prolonged laser excitation) was always observed. The amount of PL fatigue depended on excitation power and temperature. PL fatigue kinetics are described by a stretched exponential with nominal lifetimes in the 10 – 265 s range. The recovery of the PL occurred within a few seconds of light cessation. The magnitude of PL fatigue in different samples correlated with inhomogeneous line broadening of the 1.63 eV emission band, such that broader bands exhibited more fatigue. An additional luminescence band centered at 1.78 eV was observed which increased in intensity under prolonged laser irradiation. The fatigue phenomenon is tentatively attributed to two mechanisms - the formation of photo-induced defects and the formation of quasi-stable particles. Both of these mechanisms introduce additional radiative and non-radiative recombination channels that lead to a decrease in the PL intensity under prolonged laser irradiation. Since inhomogeneous line broadening and PL fatigue are related to the concentration of defects or impurities, the measurement of these two parameters is an effective method to screen sample quality.

Keywords: photoluminescence, photoluminescence fatigue, line broadening, semiconductor, quasi-stable particles, metastable defects, impurities

Introduction

The demand for efficient hard radiation detection devices for security applications as well as in medical and biomedical imaging has significantly increased in the past two decades [1,2]. An ideal gamma ray detector should have a signal output proportional to the energy deposited by the gamma ray, high efficiency (high absorption coefficient, high Z), good energy resolution, temporal stability, compact size and capability of room temperature operation [3]. Although heavy metal, wide gap semiconductors promise excellent energy-resolution for γ-ray spectroscopy, only a few systems are currently being considered because of strict demands on their optoelectronic properties. High atomic number materials such as CdZnTe, HgI_2, TlBr, PbI_2 and BiI_3 have received considerable interest [2]. In addition, thallium-based ternary compounds including Tl_6SI_4, Tl_6SeI_4, $TlGaSe_2$, Tl_3SbS_3, and Tl_2SnS_3 are being developed as potential room temperature x-ray and γ-ray detector materials [4,5]. Of these, Tl_6SeI_4 is of particular interest since mobility-lifetime ($\mu\tau$) product for charge carriers as high as 10^{-3} cm^2/V has been reported [4]. This compound crystallizes in a tetragonal structure [6], is very dense (7.38 g/cm^3) [6] and exhibits an optimal bandgap of 1.86 eV for hard radiation detection [4]. The stopping power and absorption coefficient for γ-rays for Tl_6SeI_4 are higher than those for CdZnTe, leading to an attenuation length for ^{57}Co γ radiation of only 0.4 mm at 122 keV, compared to 1.5 mm for CdZnTe [4,7].

Radiation detection efficiency also depends on material perfection. Electrically active defects are particularly important because they influence both carrier mobility and recombination lifetime by acting as scattering and recombination centers as well as trapping centers. Previously recombination centers have been observed in Tl_6SeI_4 prepared by the Bridgman crystal growth technique [8,9]. Photoluminescence (PL) measurements of Tl_6SeI_4 single crystals revealed a

broad emission band centered at 1.61 eV at 10 K, which was attributed to a donor-acceptor pair (DAP) recombination [9]. This band shows inhomogeneous line broadening with a full width at half maximum (FWHM) of 112 meV [9]. Based on density functional theory (DFT) calculations the observed emission was attributed to an antisite pair (I_{Se}-Se_I), whose formation involves an interchange of the positions of a Se ion with its nearest-neighbor I ion [10]. Detailed investigation into electronic structure, phase diagram, and dielectric, optical, and defect properties of Tl_6SeI_4 by DFT revealed that other native defects are stable including vacancies and antisites. [10].

The dominant 1.61 eV emission band shows considerable inhomogeneous line broadening [9]. Such line broadening has been previously attributed to point defects in concentrations exceeding ~1 ppm [11,12]. A semi-classical model previously developed by Morgan [13], Stern [14] and Breitenstein [15] attributed this line broadening to fluctuations in the impurity electronic band width. This model is based on an approximation that the width and skewness of the impurity band determine the shape of the emission line [13]. Furthermore, Morgan [13] and Kane [16] showed that the line broadening of a PL emission band increases with increasing total ionized luminescent defect concentration. This model has been used to correlate PL band width with ionized defect concentration in other widegap semiconductors such as *n*-GaN films doped with Si [11,17]. An increase in the donor concentration in GaN from 10^{15} to 10^{20} cm^{-3} was accompanied by a monotonic increase of FWHM of the near-band-gap emission from 18 meV to 120 meV. This line broadening was explained in terms of potential fluctuations caused by random distribution of donor impurities. Similarly, in ZnO crystals [18] and Te-doped GaSb [19] the luminescence peak broadening was ascribed to a high concentration of native

point defects. In the alloy $Cd_{1-x}Zn_xTe$, line broadening of the a bound exciton emission line, however, was attributed to compositional variation [20].

Many wide gap semiconductors under steady-state laser excitation undergo a reduction in PL emission intensity (PL fatigue) [21]. PL fatigue is observed in amorphous As_2S_3 and As_2Se_3 [22], polycrystalline CdTe/CdS solar cells [23], chalcogenide glasses [24], ZnSe [25], CdI_2 crystals doped with Ag or Cd [26], amorphous Si [27,28] and other systems [29,30,31], and has been attributed to stable or metastable photo-induced defect formation. In these cases, the luminescence is quenched through the formation of competing nonradiative recombination centers under light illumination. In contrast, PL fatigue in glass, thin films and crystals of $GeSe_2$ [32-34] was attributed to the creation of quasi-stable particles such as self-trapped excitons that enhance the rate of non-radiative recombination.

The current study is the first account of PL fatigue in Tl_6SeI_4 single crystals. Measurement of PL of Tl_6SeI_4 crystals revealed emission band centered at 1.63 ± 0.02 eV whose magnitude decreased with high optical excitation. The results indicate that PL fatigue of the 1.63 eV band is always present, prompting a closer examination of this behavior to determine its origin and ultimately implications for semiconductor detector performance. It is desirable to have a quick non-destructive screening procedure to effectively identify promising samples within as-grown ingots, and provide feedback on crystal defects and impurities. A systematic study with a focus on PL fatigue can potentially serve as a method for screening high-quality gamma ray detector materials. A correlation was established between PL fatigue of this band and its inhomogeneous line broadening, with narrower lines exhibiting lower PL fatigue. Both inhomogeneous line broadening and PL fatigue are attributed to defects which distort the local

lattice. The current approach of measuring temporal stability and FWHM of the PL emission band enables assessment of sample optical quality in a non-destructive manner.

Methods

Synthesis and Crystal Growth. The Tl_6SeI_4 samples were prepared from Tl metal (99.999% wt., Alfa Aesar), Se (pellets, 99.999% wt., Alfa Aesar) and TlI (beads 99.999% wt., Alfa Aesar) in the stoichiometric ratio. Up to 10 g of materials was placed into carbon-coated, tapered fused silica ampoules (8 mm ID, 1 mm wall thickness and 200 mm in length) and sealed under vacuum ($\sim 5\times10^{-4}$ Torr). The samples were heated to 550°C over 24 hours, held there for 12 hours, and cooled to room temperature over 12 hours.

For crystal growth polycrystalline Tl_6SeI_4 was placed in an ampoule in a two-zone Bridgman furnace equipped with a motor-controlled platform. The ampoules were embedded in thermally conductive Al_2O_3 powder in order to promote the removal of solidification heat during crystal growth. The crystal growth was performed at a speed of 0.5 $mm \cdot h^{-1}$ with a temperature gradient of 30 $^oC\ cm^{-1}$. The temperature of the hot zone was set at 600 ^oC to ensure the complete melting of Tl_6SeI_4, while the temperature for the cold zone was at 150 ^oC. After growth, the ingots were annealed at around 300 ^OC for 2 days in situ.

Post-growth Processes. The Tl_6SeI_4 wafers (~2 mm thick) were sliced perpendicular to the growth direction of ingot using a Struers Accutom-50 waferizing saw equipped with a 300 μm wide diamond-impregnated blade. The wafers were polished with silicon carbide sand paper of decreasing grit size and immediately preserved in acetone or toluene in order to avoid surface oxidation.

Annealing. A number of samples were subjected to post-growth annealing. The annealing experiments were carried out with polished sample wafers, which were sealed in a

silica tube with an inner diameter of 10 mm. In order to avoid evaporation from the wafers, which lead to surface deterioration, the samples were embedded in Tl_6SeI_4 powder. The ampoules were sealed under a vacuum of ~5×10^{-4} torr, vertically mounted into a tube furnace, and annealed at 300 ^{O}C for 24 hours. The Tl_6SeI_4 powder on the surface of wafer after annealing was washed using acetone.

Photoluminescence (PL) Measurements. The 405 nm emission line from a CW semiconductor diode laser (Excelsior One-405, Spectra-Physics) was used as the excitation source for PL measurements, with a constant power of 50 mW and a beam diameter of ~1.2 mm. The signal-to-noise ratio was increased using an optical chopper and a lock-in amplifier (SR810, Stanford Research Systems). The laser beam passed through a series of neutral optical density filters placed after the chopper in order to reduce the excitation power below 50 mW. The laser light passed through a bandpass filter (405 nm, FWHM: 10 nm, Thorlabs, Inc) prior to reaching the sample. Either a 405 nm notch filter or a 650 nm sputtered edgepass filter (Thorlabs, Inc) was used to filter the scattered and reflected laser light in front of the entrance slit to the monochromator. The absorption spectrum of the notch filter does not fully overlap on the emission spectrum of the laser, resulting in a residual second order laser line at 810 nm. The PL spectrum is resolved by a 0.75 m SPEX grating monochromator equipped with a Hamamatsu photomultiplier tube (R928 PMT). Slit widths of 200 microns for entrance and exit slits in the monochromator were used. The datasets were collected at a rate of 0.5 nm s^{-1}, such that a single PL spectrum in the 650-900 nm range can be obtained within 10 min.

The samples were mounted on a vertical stage using CRY-CON grease (Air Products and Chemicals) and cooled to cryogenic temperatures using a closed-cycle He cryostat (SHI

cryogenics DE-202). Although the grease used in mounting exhibits green luminescence under laser illumination, it is applied to the back of the sample and is not excited by the laser.

The procedure for measuring PL fatigue involved initially obtaining a PL spectrum in the 1.4-1.9 eV spectral region using laser power of 1 mW, from which data the FWHM of the peak centered at 1.63 ± 0.02 eV was obtained. The monochromator was then set to either 740 nm (1.67 eV) or 688 nm (1.70 eV) and the signal from dark noise was collected for about 10 sec without laser excitation. The monitoring wavelength is not at the peak maximum to minimize the spectral contribution from the peak at 1.52 eV. The laser was then turned on and the time decay profile was collected for a set time (at least 500 s). However, the background noise level in the PL spectrum at 50 mW is higher than that at 1 mW. Therefore, the full PL spectrum in the 1.4-1.9 eV range was obtained after PL fatigue measurements using 50 mW of laser power. Finally, the measured background level from this spectrum was subtracted from the plot of PL intensity vs time. The quoted PL fatigue lifetimes are twice the true values because the light is modulated during the PL fatigue measurement and the sample is in the dark half of excitation period.

Results

Photoluminescence

Photoluminescent properties of a series of Tl_6SeI_4 crystals were investigated. A dominant emission in the 1.62-1.69 eV range was observed in all samples consistent with the previously published results [9]. Using a laser power of 5 mW on one of the samples (**2**), the intensity of the 1.65 eV peak strongly decreased after 10 min of continuous irradiation indicative of PL fatigue (Fig. 1a). The effect of PL fatigue on the emission spectra was subsequently investigated. While at excitation powers in the range of 1-2 mW most samples exhibited a single emission band

centered at 1.63 ± 0.02 eV, the majority of samples displayed several other emission bands after prolonged irradiation using 50 mW laser power. For instance, sample **2** after etching (**2-E**) showed three overlapping bands centered at 1.52 eV, 1.65 eV, and 1.78 eV (Fig. 1b), while sample **1** exhibited only one secondary band at 1.52 eV (Fig. 1c).

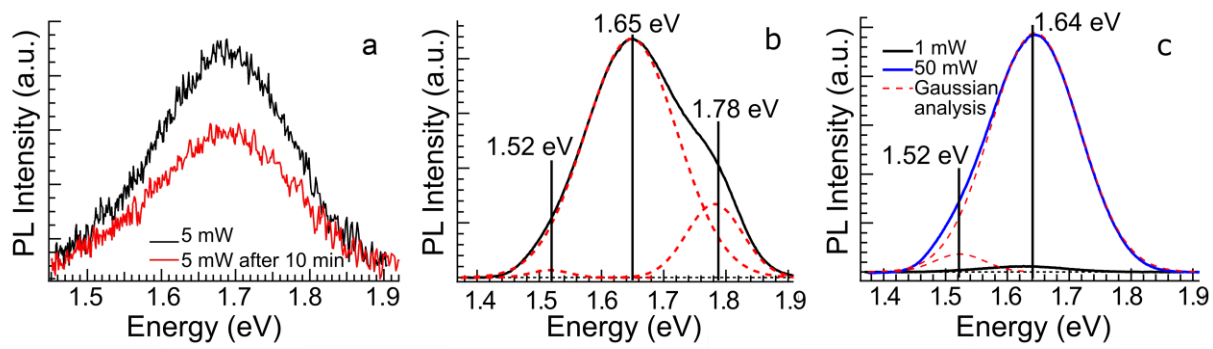

Figure 1. (a) PL spectra from a Tl_6SeI_4 sample **2** prior to polishing the surface, obtained at 16 ± 1 K, (▬) collected within the first 10 min after turning on the laser, and (▬) collected during the 10-20 min time window of continuous irradiation; PL spectra of samples (b) **2-E** and (c) **1**, collected at 17 K using (▬) 1 mW or (▬) 50 mW laser power for excitation after prolong excitation using 50 mW laser. Dashed line shows Gaussian analysis of the spectra collected using 50 mW laser power.

To determine the thermal activation energies for the peak at 1.65 eV, temperature dependence was investigated for two samples (**3** and **5**) using excitation powers of 10 mW and 1 mW, respectively. A higher laser power was used for sample **3** because it showed no evidence of PL fatigue at 10 mW, and a higher signal-to-noise ratio was obtained. The Arrhenius plot of the dependence of the integrated PL intensity on temperature for a Tl_6SeI_4 single crystal was previously analyzed using equation [9]

$$I(T) = \frac{I(0)}{1+\varphi_1 T^{3/2}+\varphi_2 T^{3/2}\exp(-\frac{E_a}{k_B T})}, \qquad (1)$$

where $I(0)$ is the extrapolated zero-temperature intensity, k_B, φ_1 and φ_2 are constants, and E_a is the thermal activation energy of a defect level. The data for samples (**5** and **3**) fit to Eq. 1 fairly well (dashed line, Fig. 2a and 2b) for the parameters $I(0)$, φ_1, φ_2, and E_a listed in Table 1.

Although the values of E_a obtained from the two data sets were the same within error (0.017 ± 0.004 eV and 0.023 ± 0.003 for **5** and **3**, respectively), they were significantly smaller than that previously reported for Tl_6SeI_4 (E_a = 0.05 ± 0.01 eV, Cho et al [9]).

The power dependence of the PL emission at low excitation power where PL fatigue does not play a role can be used to identify the underlying recombination process. Schmidt et al. [35] demonstrated that transitions due to free exciton, bound exciton, and the free-to-bound transitions can be distinguished from the excitation power dependence of the emission line intensity. The PL intensity I depends on the laser power L by the relation $I \sim L^{\gamma}$, where free- and bound-exciton emission is generally described by the γ coefficient in the $1 < \gamma < 2$ range, while for free-to-bound and donor-acceptor pair (DAP) recombination the coefficient is less than 1. Thus, the behavior of the peak at 1.65 eV under various excitation powers was investigated for sample **2** at 16 K and 57 K, and for sample **5** at 16 K. It was found that the peak intensity increased with increasing power. The plots of log (PL intensity) vs log (laser intensity) were linear with slopes in the 1.1-1.8 range indicating excitonic recombination behavior (see Supp. Info. Fig. S3).

Given that the values for γ obtained from the plots of log (PL intensity) vs log (laser power) are in the $1 \leq \gamma \leq 2$ range from three independent measurements, we explored the possibility that the emission at 1.65 eV is due to a bound exciton recombination and not DAP recombination as previously ascribed [9]. The thermal ionization of the bound exciton can be analyzed from a plot of emission intensity at different temperatures according to equation

$$I(T) = \frac{I(0)}{1 + C_1 \exp\left(-\frac{E_1}{k_B T}\right) + C_2 \exp\left(-\frac{E_2}{k_B T}\right)}, \qquad (2)$$

where E_1 and E_2 are activation energies, and C_1 and C_2 are constants. Analysis of plots of integrated PL intensity vs 1000 / T revealed that for both samples, the data fit to Eq. 2 reasonably

well (Fig. 2a and 2b, solid line). The values of E_1 and E_2 are 0.025 eV and 0.003 eV, respectively, and were the same within error from both samples (Table 1). In addition, the data from ref. [9] was re-analyzed using Eq. 2 and yielded the same values of E_1 and E_2 yet again, although the errors in the fitting parameters are notably larger (Table 1).

Table 1. The values of fitting parameters obtained from the analysis of the plots of integrated PL intensity vs. 1000/T to either Eq. 1 or Eq. 2, for the two samples of Tl_6SeI_4. The values are compared to the published data re-analyzed to Eq. 1 and 2 to obtain all variables with their corresponding errors.

Parameter	**Sample 5**	**Sample 3**	**Sample a [9]**
I(0) (a.u., 10^{-6}) (eq. 1)	1.56 ± 0.09	2.03 ± 0.07	32.6 ± 0.8
φ_1 (eq. 1)	0.0025 ± 0.0008	0.0049 ± 0.0005	0.0008 ± 0.0001
φ_2 (eq. 1)	0.12 ± 0.09	0.5 ± 0.3	0.4 ± 0.6
E_a (eV) (eq. 1)	0.017 ± 0.004	0.023 ± 0.003	0.052 ± 0.015
I(0) (a.u., 10^{-6}) (eq. 2)	1.37 ± 0.03	2.1 ± 0.5	50 ± 200
C_1 (eq. 2)	160 ± 150	600 ± 200	80 ± 200
C_2 (eq. 2)	4 ± 4	2.3 ± 0.2	1 ± 7
E_1 (eV) (eq. 2)	0.024 ± 0.007	0.025 ± 0.002	0.031 ± 0.008
E_2 (eV) (eq. 2)	0.007 ± 0.003	0.003 ± 0.001	0.001 ± 0.004

An increase in FWHM and a 50 meV blueshift of the 1.65 eV peak with increasing temperature was also observed (Fig. 2c). The temperature dependence of the FWHM of excitonic emission peaks is given by [36]

$$\Gamma(T) = \Gamma_{inh} + \gamma_{LA} T + \frac{\Gamma_{LO}}{\exp\left(\frac{\hbar\omega_{LO}}{k_B T}\right) - 1} \qquad (3)$$

where Γ_{inh} is a temperature-independent inhomogeneous broadening term, γ_{LA} is a coefficient describing the exciton-acoustic phonon contribution, Γ_{LO} is the exciton-LO phonon coupling constant, and $\hbar\omega_{LO}$ is the LO-phonon energy. The plot of FWHM vs. T agrees with Eq. 3 quite well with parameters Γ_{inh} = 182 ± 5 meV, γ_{LA} = 0.3 ± 0.3 meV/K, Γ_{LO} = 80 ± 30 meV, and $\hbar\omega_{LO}$ = 9 ± 5 meV (Fig. 2c).

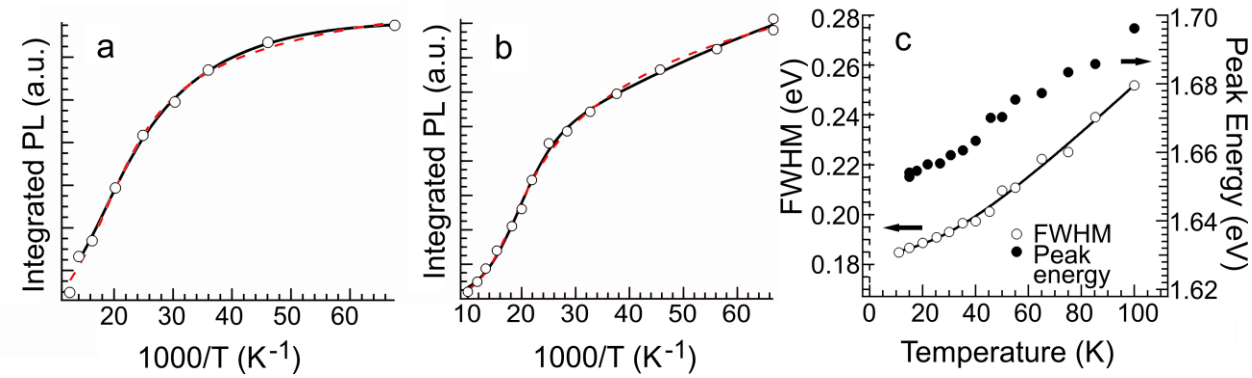

Figure 2. Plots of integrated PL intensity vs 1000 / T for sample (a) **5**, obtained from data shown in Fig. S1a, and (b) **3**, obtained from data shown in Fig. S2a. Dashed lines are the least squares analysis of the data to eq. 1, while the solid lines are the least squares analysis of the data to eq. 2. (c) A plot of FWHM (left axis) and peak energy (right axis) vs T for sample **3**, where the solid line is the least squares analysis of the data to Eq. 3.

PL Fatigue and Line Broadening

PL fatigue was observed in all samples but the degree of fatigue behavior varied depending on the sample. The magnitude of PL fatigue is described by the relative saturated intensity parameter I_∞/I_0, where I_0 is the initial PL intensity at time t = 0 s, and I_∞ is the PL intensity at infinite time (Fig. 3a). A value of unity indicates there is no PL fatigue, whereas a value of zero means that the signal completely decays within the given timeframe. The inhomogeneous line broadening given by the FWHM of the emission peak at 1.63 ± 0.02 eV also varied from sample to sample. A plot of the relative saturated value of PL fatigue vs FWHM for this peak (Fig. 3b) reveals that the data points follow two linear trends with slopes of -0.017 ± 0.003 and -0.0156 ± 0.0006 meV^{-1}, respectively, which are the same within error. The y-intercepts are 160 and 220 meV, respectively. The samples shown by data points (○) have been purified by zone refining after growth, while those shown by data points (●) were not purified after growth.

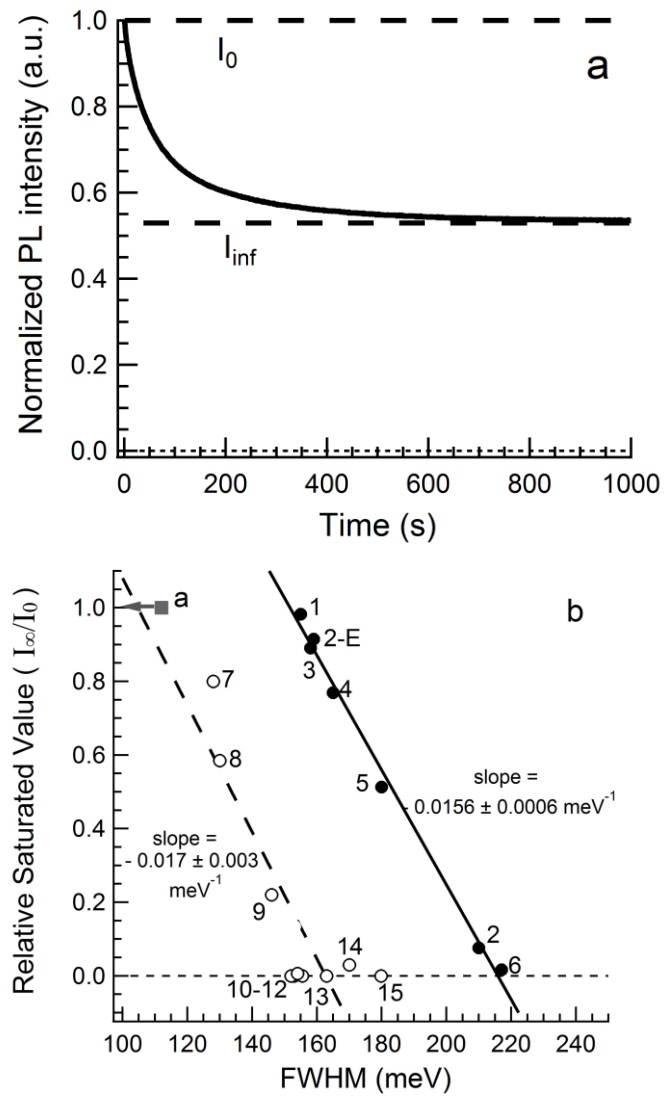

Figure 3. (a) A plot of normalized PL intensity vs. time measured at 1.67 eV for sample **5**, from which the relative saturated value is derived. (b) A plot of I_∞/I_0 vs FWHM for Tl_6SeI_4 measured at 17 ± 1K, (■) - estimated value from ref. [9], based on observation that no PL fatigue was detected upon irradiation of sample with 18 mW laser power. The two lines are the linear least squares analysis of the two data sets (●) and (○) (see text).

To determine the nature of the factors influencing PL fatigue the time-dependence of the PL intensity of the peak centered at 1.63 ± 0.02 eV was examined. The Tl_6SeI_4 sample from which the results of Fig. 1a were obtained was preserved in acetone for several weeks before the measurement. Since Tl_6SeI_4 undergoes slow oxidation in air, the sample was etched in 2% HCl for 2 min in order to remove surface oxidation and the PL measurements were subsequently

repeated. Plots of PL intensity (measured at 1.67 eV to reduce spectral overlap with the peak at 1.52 eV) vs time collected under 50 mW laser irradiation (Fig. 4) revealed that the magnitude of PL fatigue reduced by 80% as a result of etching. The reduction in PL fatigue was accompanied by concurrent narrowing of the FWHM of the 1.65 eV emission from 210 meV to 159 meV. Similarly, cleaving the sample immediately prior to PL measurement also resulted in a reduced fatigue and FWHM of the peak. Therefore, to minimize the effects of surface oxidation all other samples of Tl_6SeI_4 were polished within a few days before PL measurements and stored in toluene or acetone.

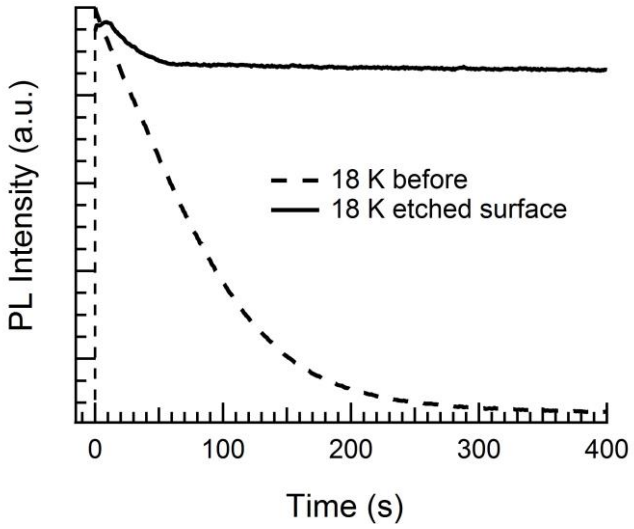

Figure 4. Plots of PL Intensity vs time at 1.67 eV for a Tl_6SeI_4 sample (**2**) under 50 mW laser irradiation collected (--) before etching (**2**), and (**—**) after etching the surface (**2-E**).

The kinetics of PL fatigue of the 1.63 ± 0.02 eV peak were investigated at 17 ± 1 K using 50 mW, 405 nm laser excitation for several independently grown Tl_6SeI_4 crystals. The fatigue kinetics are described by a stretched exponential given by [25,28]

$$I(t) = I_\infty + (I_0 - I_\infty)\exp(-\alpha t^\beta) \qquad (4)$$

where I(t) is the PL intensity at time t, I_0 and I_∞ are the intensities at the initial and infinite irradiation time, α and β are constants. The value of β is 1 for first order kinetics and 2 for second order kinetics and

$$\alpha = (1/\tau)^{\beta} \quad (5)$$

The plots of PL intensity vs irradiation time agree reasonably well with Eq. 4 in most cases, yielding a lifetime of PL fatigue (τ_F) in the 10 – 265 s range and β-value varied between 0.6 and 1.9. This variation in the magnitude of the parameter β likely indicates that there are multi-activation energy processes that give rise to PL fatigue. It should be noted that the analysis was sometimes complicated by the presence of concurrent growth/decay processes in the PL intensity vs irradiation time plots. In addition, the PL fatigue profile of a few samples was superimposed on a slow decaying tail which also complicated the analysis of the data to Eq. 4. As a consequence, the as-measured τ_{PL} values did not correlate with other optical properties, such as FWHM of the peaks or PL emission intensities.

Recovery Lifetime of PL Fatigue

Excitation at a high laser power resulted in formation of an additional peak at 1.78 eV in several samples. The PL intensity of this peak under continuous excitation was investigated by performing an "ON-OFF" experiment on one sample with a low FWHM and minimal fatigue (Fig. 5a). The sample was monitored at 1.80 eV to reduce the spectral overlap between the two bands at 1.63 ± 0.02 and 1.78 eV. The light was switched ON for approximately 100 secs, during which time a growth and decay profile of the PL intensity was observed (Fig. 5b, 'initial'). The laser was subsequently turned off for 256 s and the PL fatigue was measured again (Fig. 7b, 't_{dark} = 256s'). A substantial recovery of both the growth and the decay portion of the PL intensity-time curve was observed (the recovered signal intensity is given by I(recovery)). This cycle was repeated three times with varying t_{dark} intervals ('OFF' intervals). The results show that when the t_{dark} is short (10 s and 37 s) only an exponential decay dependence is observed. When the t_{dark} is much longer (256 s), overlapping growth and decay curves are observed (Fig. 5b).

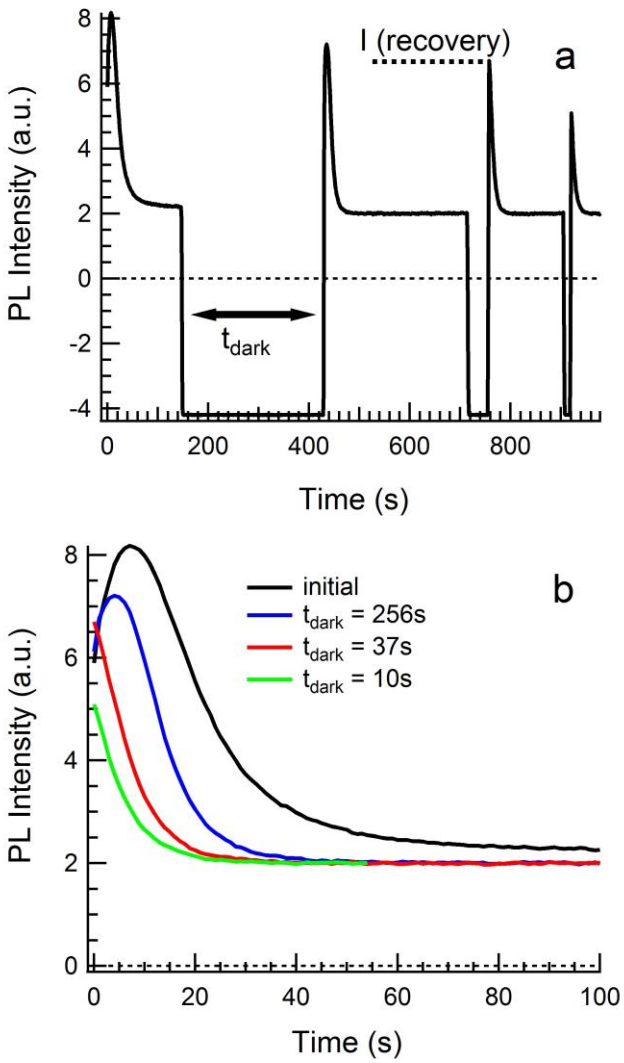

Figure 5. (a) Plot of PL intensity vs time measured at 1.80 eV during the "ON-OFF" experiment for sample **2-E**, collected using 50 mW laser power at 17 K. The signal has been corrected for background noise (see experimental section). (b) Overlaid PL fatigue data from (a) after various dark intervals.

To determine the recovery time (τ_{RF}) of the PL emission at 1.63 ± 0.02 eV after turning off the laser, an 'ON-OFF' experiment was performed at different temperatures on samples **1** and **16** as described above. Only a decay profile on a PL intensity-time plot was observed at 1.67 eV, in contrast to the 1.78 eV peak that showed both a growth and a decay portions. The fraction of signal fatigue (FSF) parameter is given by the $(I_0\text{-}I(recovery))/I_0$ ratio, where I_0 and I(recovery) are the initial and recovered signal intensity, respectively. Plots of FSF vs t_{dark} for samples **1** and

16 indicate that τ_{RF} increases with increasing temperature for sample **1**, while that for **16** is independent of temperature (Fig. 6a and 6b). In both cases, the plots follow stretched exponential in time analogous to Eq. 4, given by

$$FSF(t_{dark}) = \exp(-\alpha \cdot t_{dark}{}^{\beta}) . \qquad (6)$$

Using Eq. 5, τ_{RF} for sample **16** was 92 s, while that for sample **1** increased from ~2 s to 12 s with increasing temperature (Fig. 6c).

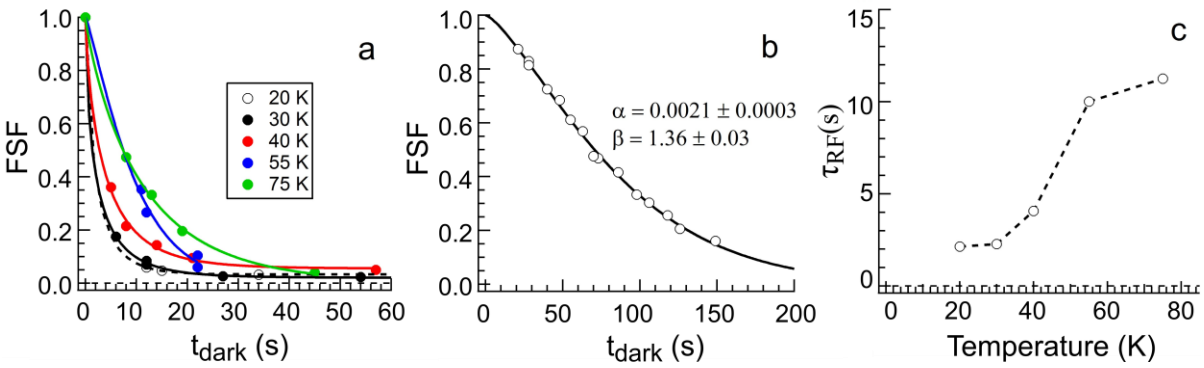

Figure 6. Plots of Fraction of Signal Fatique (FSF) vs t_{dark} determined from the "ON-OFF" experiments at different temperatures for samples (a) **1** and (b) **16**, the solid line is the fitting of data to Eq. 6. The plot in (b) was obtained from temperatures in the 12-40 K range, since in that temperature range the data showed no variation. (c) Plot of PL fatigue recovery lifetime vs T for sample **1**, determined from fitting of the data in (a) to Eq. 6 and 5.

Temperature and Power Dependence on PL fatigue

To better understand factors responsible for PL fatigue, the dependence PL fatigue kinetics on laser power and temperature was investigated on Tl_6SeI_4 single crystals. PL intensity vs irradiation time profiles were examined under continuous excitation with laser power in the 15.8-50 mW range for sample **16** at 12 K (Fig. S9c, Supp. Info). The results indicate that the initial signal intensity (I_0) decreased with decreasing laser power, since fewer carriers are generated with a lower laser power. This was accompanied by an increase in the saturation emission intensity level (I_∞), leading to an enhancement in the relative saturated value with a reduction of laser power (Fig. 7a, right axis). The measured decay profile of PL fatigue agrees

with Eq. 4 at each power, revealing that as the laser intensity increased from 15.8 mW to 50 mW, the lifetime of PL fatigue (τ_F) decreases from 75 s to 30 s approaching a plateau region (Fig. 7a, left axis).

Examination of PL intensity vs time profiles at temperatures in the 12 – 75 K range for the two samples (**16** and **1**) revealed that the PL fatigue characteristics depend on sample. For **16**, the I_0 value reduced with increasing temperature, while the value of I_∞/I_0 remained nearly constant (Fig. S9b). On the other hand, both I_0 and I_∞ reduced systematically with increasing temperature for sample **1** (Fig. S9a). The plots of PL fatigue lifetime vs temperature show that the temperature dependence also differs for the two samples. As such, the PL fatigue lifetime of sample **16** decreases with increasing temperature, while a modest increase between 12 K and 40 K is followed by a decrease in the PL fatigue lifetime in sample **1** (Fig. 7b). A plot of the temperature dependence of Relative Saturated Value (I_∞/I_0) and FWHM of the peak at 1.65 eV for sample **1** shows that an increase in temperature is accompanied by a decrease in the I_∞/I_0 value and an increase in the FWHM value (Fig. 7c).

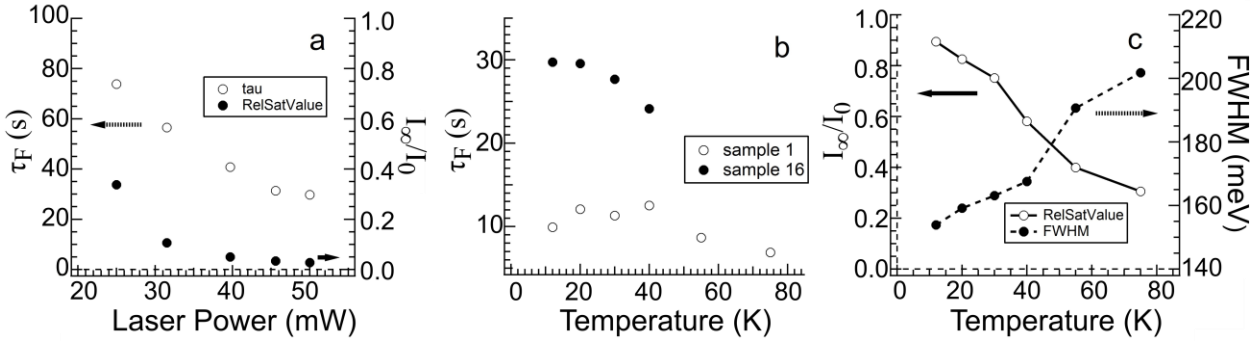

Figure 7. (a) Plots of lifetime of PL fatigue (○, left axis) and Relative saturated value (●, right axis) vs laser power, for sample **16**; (b) plots of lifetime of PL fatigue vs temperature, for (○) **1** sample, and (●) **16** sample; (c) Plots of Relative Saturated Value (○, I_∞/I_0, left axis) vs T, and FWHM (●, right axis) vs T, for PL of sample **1**.

Discussion

a. Photoluminescence Fatigue and Recovery

PL fatigue was observed in all cases but the degree varied between samples (Fig. 3b). Phenomena that can lead to PL fatigue in semiconductors have been widely studied and include light-induced defect formation [23,25,27-30,31,37] and quasi-stable particle formation [32-34]. Both of these phenomena enhance non-radiative recombination rate, thus suppressing the PL emission intensity. In Tl_6SeI_4 the decrease of laser power resulted in the increase of the ratio I_∞/I_0 as well as an increase in τ_F (Fig. 7a). Both above-mentioned mechanisms will lead to this observation, indicating that the processes responsible for PL fatigue are faster at higher excitation power and thus quench luminescence more efficiently.

In Tl_6SeI_4 single crystals, the "ON-OFF" experiment indicates that τ_{RF} at 20 K for samples **16** and **1** is 92 s and 2 s, respectively (Fig. 6a and 6b). In the cases where PL fatigue is caused by photo-induced defects (GaN epilayers[29], amorphous Si[30,37] and Ge_xSe_{1-x}[31], and ZnSe[25]) the PL signals can usually be restored either by heating or by infrared irradiation of the samples. A notable exception is PL fatigue in polycrystalline CdTe/CdS solar cells [23], where PL signals are restored within 30 s in the dark at low temperature. In comparison, if the PL fatigue is due to the formation of quasi-stable particles as is the case in glassy[32,33] and crystalline[33] $GeSe_2$, a recovery of PL fatigue in the dark at low temperature is observed within 25 s [32-34]. Given the rapid PL signal recovery in the dark at low temperature of Tl_6SeI_4, our results are largely consistent with the formation of quasi-stable particles (i.e. self-trapped excitons [38]), however photo-induced defect formation cannot be ruled out.

The PL fatigue behavior observed in Tl_6SeI_4 samples depends on temperature. For sample **1** the I_∞/I_0 ratio decreased with increasing temperature, while that for sample **16** was

independent of temperature and decreased with decreasing laser power. Furthermore, the τ_{RF} for sample **1** increases with increasing temperature (Fig. 6c) and is consistent with the temperature dependence of the I_∞/I_0 ratio. As the temperature is increased, the amount of PL fatigue increases (given by the I_∞/I_0 ratio) and thus a longer dark interval is required to fully recover the PL signal. The temperature dependent behavior of sample **1** can be compared to a similar behavior reported for polycrystalline CdTe/CdS solar cells [23] and $GeSe_2$ single crystals [33]. In both of those cases, temperature dependent studies on PL fatigue revealed that the I_∞/I_0 ratio decreases with increasing temperature analogous to that observed for Tl_6SeI_4 in this study (Fig. 7c). The observed phenomenon in CdTe/CdS solar cells [23] was attributed to defect creation under illumination, while in $GeSe_2$ single crystals quasi-excitons are thought to be involved [33]. Furthermore, PL fatigue lifetime decreased with increasing temperature (Fig 7b), presumably due to the increase in thermally activated defect or impurity centers which enhance the rate of metastable particle or defect formation at higher temperatures. Therefore, our results are consistent with both models involving either photo-induced defect or quasi-stable particle formation.

The light-induced defect formation is analogous to DX centers observed in III-V semiconductors[39], where a highly localized and charged deep level defect results from significant lattice distortion. Continuous photoexcitation causes this defect to transform into a shallow excited state, which is metastable. Evidence for the formation of photo-induced defects was obtained for Tl_6SeI_4 from the "ON-OFF" experiment, where an additional peak at 1.80 eV was observed to grow under continuous excitation (Fig. 5). Similarly, an additional photoinduced radiative recombination in GaN was attributed to the creation and/or filling of a metastable state [29,40]. In Tl_6SeI_4 crystals, there is an overlap at 1.80 eV between two bands centered at 1.65 eV

(deep level) and 1.78 eV (shallow metastable level) (Fig. 1b). Since the 1.65 eV peak decays with time (Fig. 3a), it follows that the increase of the PL signal at 1.80 eV is due to the band at 1.78 eV. The observed subsequent decay of the emission-time profile at 1.80 eV is due to the decay of the overlapping band at 1.65 eV. The "ON-OFF" experiment indicates that while the decay portion of the emission-time profile recovers within seconds of the "OFF" period, it takes minutes for the recovery of the growth process to occur. This observation suggests that two separate processes are taking place with different timescales, for example competing radiative and non-radiative recombination processes.

b. Surface oxidation

The effects of surface oxidation of PL fatigue and FWHM were also investigated. The results indicate that freshly cleaved or chemically etched samples show narrower peaks and less PL fatigue compared to samples which were exposed to air for several weeks (Fig. 4). This finding suggests that the PL fatigue in Tl_6SeI_4 may be partly caused by surface oxidation, which can be removed by etching the surface. We propose that oxidation leads to the formation of photoinduced non-radiative recombination channels that compete with radiative emission, lowering the quantum yield of the PL intensity.

c. Inhomogeneous Line Broadening (FWHM)

Although all Tl_6SeI_4 samples measured in the current study exhibited an emission peak centered at 1.63 ± 0.02 eV, the peak width and PL fatigue varied significantly among samples. This variation in PL fatigue suggests differences in the concentration of defects (native or extrinsic) that result in the formation of either metastable quasi-stable particles (e.g. self-trapped excitons) or defects induced by light. These defect states enhance non-radiative recombination according to the configuration coordinate diagram shown in Fig. 8 [32,41]. At low excitation the

absorption of photons from A → B results in a radiative recombination C → D. However, at higher excitation and continuous irradiation, photoinduced defects or quasi-stable particles are formed and some transition to a metastable state (M) [transition G → M], which is in equilibrium with the ground state (G). It is proposed that the onset of state M introduces new non-radiative recombination channels along path 2 and results in the observed PL fatigue. Upon cessation of the excitation, the localized metastable states created by the high laser power decays spontaneously and the system returns to its original state [transition M → G]. The concentration of the metastable defect sites is dependent on the number of defect/impurity centers. Thus, it is expected that lower fatigue would be present in crystals with low concentration of defect/impurity centers since less metastable states would be formed. The plot of I_∞/I_0 value of fatigue vs FWHM of the peak at 1.63 ± 0.02 eV suggests that there is a linear relationship between the two variables (Fig. 3b). As previously discussed, defects present in high concentrations cause line broadening of the PL peaks [11-15,42]. Therefore, we propose that in Tl_6SeI_4 crystals the difference in FWHM of the 1.63 ± 0.02 eV emission is due to a variation in defect emission line widths. Since the I_∞/I_0 ratio is also dependent on the number of defect/impurity centers, a correlation between FWHM and the I_∞/I_0 ratio is expected. Such a correlation is observed as shown in Fig. 3b. However, this plot shows that the data points fall on two different lines, offset by ~53 meV. Since samples (○) were zone refined after compound synthesis, it could have resulted in a partial removal of defects responsible for band broadening while not affecting PL fatigue.

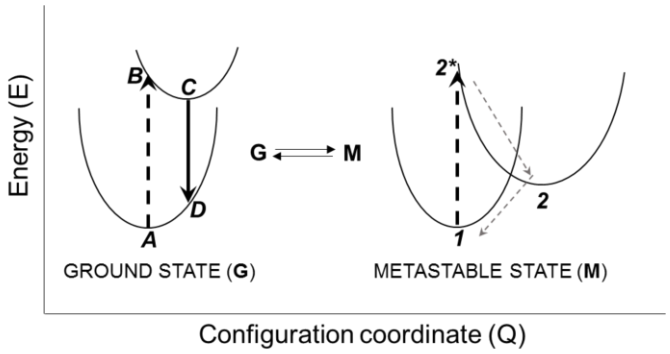

Figure 8. Configuration coordinate diagram showing radiative transitions in the ground state and non-radiating recombination paths in the metastable state (see text).

Summary and Conclusions

All samples of Tl_6SeI_4 exhibit a PL band centered at 1.63 ± 0.02 eV that is attributed to bound exciton emission. The band showed photoluminescence decay under high intensity laser excitation, whose kinetics followed stretched exponential time decays. PL fatigue was observed that decreased with increasing laser power, such that at 1 mW laser power no PL fatigue is observed in Tl_6SeI_4 samples. The associated lifetime for PL fatigue decreased at higher excitation power, indicating that the rate of the process responsible for quenching of PL emission is proportional to laser power. In addition, the I_∞/I_0 ratio describing the amount of PL fatigue depended on temperature, resulting in more pronounced fatigue behavior at higher temperatures. A correlation between inhomogeneous line broadening and PL fatigue was established, such that samples with minimal PL fatigue showed narrower band widths. The variation in the line widths of PL emission is related to impurity or defect concentration, where samples with low concentration of defects show narrower line widths. The plots of PL fatigue vs FWHM for two series of samples followed two distinct linear curves. PL fatigue was attributed to two mechanisms: the formation of metastable point defects and the formation of quasi-stable particles. Both of these mechanisms depend of the concentration of defects that distort the local

band structure and introduce additional radiative or non-radiative recombination channels. The measurements of FHWM and PL fatigue can therefore provide an effective non-destructive technique to assess the crystal quality of the as-grown crystals.

Acknowledgements

This work was supported by the Department of Homeland Security with grant DN-077-ARI086-01, and the National Nuclear Security Administration with grant DE-NA0002522. The authors would like to thank Dr. Micah P. Hanson for technical discussions.

References

1 G. F. Knoll, *Radiation Detection and Measurement*. (Wiley, Hoboken, NJ, 2010), 4th ed; S. Del Sordo, L. Abbene, E. Caroli, A. M. Mancini, A. Zappettini, and P. Ubertini, *Sensors* **9** (5), 3491-3526 (2009); A. Owens and A. Peacock, *Nucl. Instrum. Methods Phys. Res., Sect. A* **531** (1–2), 18-37 (2004); A. Owens, *J. Synchrotron Radiat.* **13** (2), 143-150 (2006); R. Devanathan, L. R. Corrales, F. Gao, and W. J. Weber, *Nucl. Instrum. Methods Phys. Res., Sect. A* **565** (2), 637-649 (2006).

2 A. Owens, *Compound Semiconductor Radiation Detectors*. (Taylor & Francis, 2012).

3 G. Gilmore, *Practical Gamma-Ray Spectrometry*. (Wiley, Chichester, England, Hoboken, NJ, 2008), 2nd ed.. ed; D. Reilly, N. Ensslin, J. Hastings Smith, and S. Kreiner, *Passive Nondestructive Assay of Nuclear Materials*. (Office of Nuclear Regulatory Research, Washington, DC, 1991).

4 S. Johnsen, Z. Liu, J. A. Peters, J.-H. Song, S. Nguyen, C. D. Malliakas, H. Jin, A. J. Freeman, B. W. Wessels, and M. G. Kanatzidis, *J. Am. Chem. Soc.* **133** (26), 10030-10033 (2011).

5 S. L. Nguyen, C. D. Malliakas, J. A. Peters, Z. Liu, J. Im, L.-D. Zhao, M. Sebastian, H. Jin, H. Li, S. Johnsen, B. W. Wessels, A. J. Freeman, and M. G. Kanatzidis, *Chem. Mater.* **25** (14), 2868-2877 (2013); Z. Liu, J. A. Peters, B. W. Wessels, S. Johnsen, and M. G. Kanatzidis, *Nucl. Instrum. Methods Phys. Res., Sect. A* **659** (1), 333-335 (2011); Z. Liu, J. A. Peters, C. Zang, N. K. Cho, B. W. Wessels, S. Johnsen, S. Peter, J. Androulakis, M. G. Kanatzidis, J.-H. Song, H. Jin, and A. J. Freeman, *Proc. SPIE* **8018**, 80180H (2011); S. Johnsen, Z. Liu, J. A. Peters, J.-H. Song, S. C. Peter, C. D. Malliakas, N. K. Cho, H. Jin, A. J. Freeman, B. W. Wessels, and M. G. Kanatzidis, *Chem. Mater.* **23** (12), 3120-3128 (2011); Z. Liu, J. A. Peters, S. Nguyen, M. Sebastian, B. W. Wessels, S. Wang, H. Jin, J. Im, A. J. Freeman, and M. G. Kanatzidis, *Proc. SPIE* **8507**, 85070O (2012); S. Wang, Z. Liu, J. A. Peters, M. Sebastian, S. L. Nguyen, C. D. Malliakas, C. C. Stoumpos, J. Im, A. J. Freeman, B. W. Wessels, and M. G. Kanatzidis, *Cryst. Growth Des.* **14** (5), 2401-2410 (2014); H. Kim, L. Cirignano, A. Churilov, G. Ciampi, A. Kargar, W. Higgins, P. O'Dougherty, S. Kim, M. R. Squillante, and K. Shah, *Proc. SPIE* **7806**, 780604-780604-780613 (2010); M. Kocsis, *IEEE Trans. Nucl. Sci.* **47** (6), 1945-1947 (2000); N. S. Yuksek, H. Kavas, N. M. Gasanly, and H. Ozkan, *Physica B* **344** (1–4), 249-254 (2004).

6 R. Blachnik, H. A. Dreisbach, and J. Pelzl, *Mater. Res. Bull.* **19** (5), 599-605 (1984).

7 S. M. Seltzer, *Radiat. Res.* **136** (2), 147-170 (1993).

8 Z. Liu, J. A. Peters, M. Sebastian, M. G. Kanatzidis, J. Im, A. J. Freeman, and B. W. Wessels, *Semicond. Sci. Technol.* **29** (11), 115002 (2014).

9 N. K. Cho, J. A. Peters, Z. Liu, B. W. Wessels, S. Johnsen, M. G. Kanatzidis, J. H. Song, H. Jin, and A. Freeman, *Semicond. Sci. Technol.* **27** (1), 015016-015019 (2012).

10 K. Biswas, M.-H. Du, and D. J. Singh, *Phys. Rev. B* **86** (14), 144108 (2012).

11 E. F. Schubert, I. D. Goepfert, W. Grieshaber, and J. M. Redwing, *Appl. Phys. Lett.* **71** (7), 921-923 (1997).

12 S. R. Dhariwal, V. N. Ojha, and G. P. Srivastava, *IEEE Trans. Electron Devices* **32** (1), 44-48 (1985).

13 T. N. Morgan, *Phys. Rev.* **139** (1A), A343-A348 (1965).

14 F. Stern, *Phys. Rev. B* **9** (10), 4597-4598 (1974).

15 O. Breitenstein and K. Unger, *Phys. Status Solidi B* **91** (2), 557-562 (1979).
16 E. O. Kane, *Phys. Rev.* **131** (1), 79-88 (1963).
17 E. Iliopoulos, D. Doppalapudi, H. M. Ng, and T. D. Moustakas, *Appl. Phys. Lett.* **73** (3), 375-377 (1998).
18 V. V. Ursaki, I. M. Tiginyanu, V. V. Zalamai, E. V. Rusu, G. A. Emelchenko, V. M. Masalov, and E. N. Samarov, *Phys. Rev. B* **70** (15), 155204 (2004).
19 A. S. Vlasov, E. P. Rakova, V. P. Khvostikov, S. V. Sorokina, V. S. Kalinovsky, M. Z. Shvarts, and V. M. Andreev, *Sol. Energy Mater. Sol. Cells* **94** (6), 1113-1117 (2010).
20 K. Suzuki, N. Akita, K. Inagaki, A. Nishihata, N. Takojima, and S. Dairaku, *J. Cryst. Growth* **138** (1), 199-203 (1994).
21 I. Pelant and J. Valenta, *Luminescence Spectroscopy of Semiconductors*. (Oxford University Press, New York, 2012).
22 R. A. Street, T. M. Searle, and I. G. Austin, *J. Phys. C: Solid State Phys.* **6** (10), 1830 (1973); J. Cernogora, F. Mollot, and C. B. À. La Guillaume, *Phys. Status Solidi A* **15** (2), 401-407 (1973); S. G. Bishop, B. V. Shanabrook, U. Strom, and P. C. Taylor, *J. Phys. Colloq.* **42** (C4), C4-383-C384-386 (1981); S. G. Bishop and P. C. Taylor, *Philos. Mag. B* **40** (6), 483-495 (1979).
23 D. Shvydka, C. Verzella, V. G. Karpov, and A. D. Compaan, *J. Appl. Phys.* **94** (6), 3901-3906 (2003).
24 T. Nakanishi, Y. Tomii, and K. Hachiya, *Electrochim. Acta* **100**, 304-310 (2013); T. Nakanishi, Y. Tomii, and K. Hachiya, *J. Non-Cryst. Solids* **354** (15–16), 1627-1632 (2008); M. Seki and K. Hachiya, *J. Phys.: Condens. Matter* **15** (26), 4555 (2003).
25 N. Q. Liem, J. I. Lee, V. X. Quang, D. X. Thanh, D. Kim, J.-S. Son, and S. K. Noh, *J. Cryst. Growth* **214–215** (0), 441-446 (2000).
26 I. M. Bolesta, S. R. Vel'gosh, I. D. Karbovnik, V. N. Lesivtsiv, and I. N. Rovetskii, *Phys. Solid State* **54** (10), 2061-2065 (2012).
27 I. Hirabayashi, K. Morigaki, and S. Nitta, *Jpn. J. Appl. Phys.* **19** (7), L357 (1980).
28 D. Redfield and R. H. Bube, *Appl. Phys. Lett.* **54** (11), 1037-1039 (1989).
29 S. J. Xu, G. Li, S. J. Chua, X. C. Wang, and W. Wang, *Appl. Phys. Lett.* **72** (19), 2451-2453 (1998).
30 M. Kumeda, T. Ohta, and T. Shinizu, *Solid State Commun.* **64** (3), 291-294 (1987); K. Shimakawa, A. Kondo, K. Hayashi, S. Akahori, T. Kato, and S. R. Elliot, *J. Non-Cryst. Solids* **164–166, Part 1** (0), 387-390 (1993).
31 F. Mollot, J. Cernogora, and C. Benoit àla Guillaume, *J. Non-Cryst. Solids* **35–36, Part 2** (0), 939-944 (1980).
32 V. A. Vassilyev, M. Koós, and I. Kósa Somogyi, *Solid State Commun.* **28** (8), 613-616 (1978).
33 M. Koós, I. K. Somogyi, and V. A. Vassilyev, *J. Lumin.* **26** (4), 449-462 (1982).
34 M. Koós, I. K. Somogyi, and V. A. Vassilyev, *J. Non-Cryst. Solids* **43** (2), 245-253 (1981).
35 T. Schmidt, K. Lischka, and W. Zulehner, *Phys. Rev. B* **45** (16), 8989-8994 (1992).
36 S. Rudin, T. L. Reinecke, and B. Segall, *Phys. Rev. B* **42** (17), 11218-11231 (1990).
37 M. Stutzmann, W. B. Jackson, and C. C. Tsai, *Phys. Rev. B* **32** (1), 23-47 (1985).
38 R. T. Williams and K. S. Song, *J. Phys. Chem. Solids* **51** (7), 679-716 (1990); A. M. Stoneham, J. Gavartin, A. L. Shluger, A. V. Kimmel, D. M. Ramo, H. M. Rønnow, G. Aeppli, and C. Renner, *J. Phys.: Condens. Matter* **19** (25), 255208 (2007).

39 P. M. Mooney, *J. Appl. Phys.* **67** (3), R1-R26 (1990).
40 I. K. Shmagin, J. F. Muth, J. H. Lee, R. M. Kolbas, C. M. Balkas, Z. Sitar, and R. F. Davis, *Appl. Phys. Lett.* **71** (4), 455-457 (1997).
41 N. F. Mott and A. M. Stoneham, *J. Phys. C: Solid State Phys.* **10** (17), 3391 (1977).
42 D. O. Toginho Filho, I. F. L. Dias, J. L. Duarte, E. Laureto, and J. C. Harmand, *Brazilian Journal of Physics* **35**, 999-1005 (2005).